ELSEVIER

Nuclear Instruments and Methods in Physics Research A 496 (2003) 33–43

NUCLEAR INSTRUMENTS & METHODS IN PHYSICS RESEARCH Section A

www.elsevier.com/locate/nima

Smooth approximation with acceleration in an alternating phase focusing superconducting linac

Ji Qiang[a,*], Robert W. Garnett[b]

[a] *Accelerator and Fusion Research Division, Lawrence Berkeley National Laboratory, 1 Cyclotron Road, MS 71J, Berkeley, CA 94720, USA*

[b] *Los Alamos National Laboratory, Ms H817, LANSCE-1, Los Alamos, NM 87545, USA*

Received 2 May 2002; received in revised form 1 July 2002; accepted 15 July 2002

Abstract

In this paper, we present a smooth approximation method to calculate the effective potential in a longitudinal RF accelerating and focusing system. Comparing with the smooth approximation without acceleration, this method gives a more accurate calculation of the zero-current phase advance and effective potential when the energy gain through a period is not negligible. Using such a smooth approximation, we have studied an alternating phase focusing structure in a proposed accelerator-driven test facility superconducting linac. A self-consistent macroparticle simulation for one asymmetrical alternating phase focusing structure shows that beyond a beam current of 50 mA, there will be significant particle losses. This will put a limit on the future machine operation based on the alternating phase focusing concept.

PACS: 27.27.−a

Keywords: Smooth approximation; Alternating phase focusing

1. Introduction

In the past couple of decades, Alternating Phase Focusing (APF) structures have been studied to achieve simultaneously longitudinal and transverse focusing in accelerators [1–6]. In normal-conducting accelerators like Drift-Tube Linacs (DTLs), by controlling the driven phase of the accelerating structure and the distance between the cavities, the beam can be both longitudinally stable and accelerated through the system. However, using only APF also results in a weaker transverse focusing strength with nonlinear fields, potential coupling between the transverse and longitudinal motion, and reduction of the longitudinal RF bucket size. In a superconducting linac, due to the increasing length of the lattice period and high cavity accelerating gradients, the zero-current phase advance can be greater than 90°, which may cause an envelope instability of the beam [7]. Using APF will significantly reduce the zero-current phase advance while maintaining the same energy gain. Meanwhile, adding external transverse focusing would give separate control of transverse and longitudinal beam dynamics.

The smooth approximation has been used in previous studies of APF structures [1,2,4,6,8,9]. In

*Corresponding author.
E-mail address: jqiang@lbl.gov (Ji Qiang).

0168-9002/03/$ - see front matter
PII: S0168-9002(02)01631-5

those studies, the energy gain through one acceleration period was assumed to be negligible. This assumption is valid for normal-conducting accelerators like the DTL where the accelerating gradient is low and the energy gain is small in one lattice period. In superconducting linacs, the RF cavities can have much higher accelerating gradients and the energy gain in one period may no longer be negligible. Including the effects of acceleration will affect the calculation of the effective potential in a lattice period and the calculation of the zero-current phase advance. In this paper, we will first present a smooth approximation without acceleration in Section 2. In Section 3, the smooth approximation with acceleration is presented. Application to the design of an APF superconducting linac is given in Section 4. The conclusions are drawn in Section 5.

2. Longitudinal smooth approximation without acceleration

For a charged particle moving inside an accelerator and using z as the independent variable, the general equations of motion are

$$x' = \frac{p_x}{p_z} \tag{1}$$

$$y' = \frac{p_y}{p_z} \tag{2}$$

$$\psi' = \frac{(\omega/c)\gamma}{p_z} - \frac{(\omega/c)}{\beta_0} \tag{3}$$

$$p_x' = \frac{q}{mcp_z}\left(\frac{\gamma}{c}\mathbf{E} + \mathbf{p}\times\mathbf{B}\right)_x \tag{4}$$

$$p_y' = \frac{q}{mcp_z}\left(\frac{\gamma}{c}\mathbf{E} + \mathbf{p}\times\mathbf{B}\right)_y \tag{5}$$

$$p_t' = \frac{q}{mc^2}e_0\cos(\omega t_0+\theta) - \frac{q}{mc^2p_z}\mathbf{p}\cdot\mathbf{E} \tag{6}$$

where ψ is the phase relative to the reference particle defined by $\psi = \omega(t - t_0)$, ω is the assumed RF frequency, t_0 is the flight time of the reference particle, p_t is the normalized energy deviation with respect to the reference particle, $p_t = \gamma_0 - \gamma$, where γ_0 is the γ of the reference particle, $\gamma = 1/\sqrt{1-\beta^2}$, $\beta_i = v_i/c$ with $i = x, y, z$, $\beta_0 = \sqrt{1-1/\gamma_0^2}$, $p_i = \gamma\beta_i$, c is the speed of light, m is the rest mass of the particle, θ is the initial drive phase, and the superscript prime denotes $\mathrm{d}/\mathrm{d}z$. The electric field, $\mathbf{E}$, and magnetic field, $\mathbf{B}$, include the contributions from external focusing and accelerating fields and the mean-field of intra-particle Coulomb interactions. The trajectory of the reference particle on the axis of the accelerator can be determined from the following:

$$t_0' = \frac{1}{\beta_0 c} \tag{7}$$

$$\gamma_0' = \frac{q}{mc^2}e_0(z)\cos(\omega t_0+\theta) \tag{8}$$

where e_0 is the spatial part of the on-axis external electrical field.

For an RF linac, the electromagnetic field in a cylindrically symmetric accelerating structure can be obtained from

$$\mathbf{E} = -\frac{\partial\mathbf{A}}{\partial t} \tag{9}$$

$$\mathbf{B} = \nabla\times\mathbf{A} \tag{10}$$

where the vector potential is given by [10]

$$A_x = \frac{1}{\omega}x\sum_{n=0}^{\infty}\frac{1}{2(n+1)}e_n'(z)r^{2n}\sin(\omega t+\theta) \tag{11}$$

$$A_y = \frac{1}{\omega}y\sum_{n=0}^{\infty}\frac{1}{2(n+1)}e_n'(z)r^{2n}\sin(\omega t+\theta) \tag{12}$$

$$A_z = -\frac{1}{\omega}\sum_{n=0}^{\infty}e_n'(z)r^{2n}\sin(\omega t+\theta) \tag{13}$$

with $r^2 = x^2 + y^2$ and

$$e_{n+1} = -\frac{1}{4(n+1)^2}\left(e_n''(z) + \frac{\omega^2}{c^2}e_n(z)\right). \tag{14}$$

In an APF superconducting linac design, it is very important to know the bucket size since it relates to the longitudinal RF focusing. For a periodic structure, the smooth approximation can be used to find the effective potential of the RF field. The RF bucket size, i.e. phase acceptance and the energy width, can be obtained from the effective potential. Neglecting the energy change through the lattice period, the calculation

of the effective potential can be drastically simplified. A closed form of the effective potential as a function of phase can be derived. From now on, we will consider only the dynamics of particles on the axis. Without space-charge forces, the equations of motion can be rewritten as

$$\psi' = \frac{\omega}{c}\frac{p_t}{\gamma_0^3\beta_0^3} \tag{15}$$

$$p_t' = -\frac{q}{mc^2}F(z,\psi) \tag{16}$$

where

$$F(z,\psi) = \sum_i e_{0i}(z)(\cos(k_0 z + \theta_i + \psi) - \cos(k_0 z + \theta_i)). \tag{17}$$

In above equation, e_{0i} is the field amplitude on the axis for the ith cavity, θ_i is the driven phase for the ith cavity, the wave number $k_0 = 2\pi/\beta_0\lambda$, and the wavelength $\lambda = 2\pi c/\omega$. For a lattice period L, we can expand the function F by Fourier series as

$$F(z,\psi) = \frac{1}{2}a_0(\psi) + \sum_{n=1}^{\infty} a_n(\psi)\cos\left(k_L n\left(z-\frac{L}{2}\right)\right) + \sum_{n=1}^{\infty} b_n(\psi)\sin\left(k_L n\left(z-\frac{L}{2}\right)\right) \tag{18}$$

where $k_L = 2\pi/L$ and

$$a_n(\psi) = C_{1n}\cos(\psi) - C_{2n}\sin(\psi) - C_{1n} \tag{19}$$

$$b_n(\psi) = S_{1n}\cos(\psi) - S_{2n}\sin(\psi) - S_{1n}. \tag{20}$$

The coefficients C_{1n}, C_{2n}, S_{1n}, and S_{2n} are given by

$$C_{1n} = \frac{2}{L}\int_0^L \sum_i e_i(z)\cos(k_0 z + \theta_i) \times \cos\left(k_L n\left(z-\frac{L}{2}\right)\right) dz \tag{21}$$

$$C_{2n} = \frac{2}{L}\int_0^L \sum_i e_i(z)\sin(k_0 z + \theta_i) \times \cos\left(k_L n\left(z-\frac{L}{2}\right)\right) dz \tag{22}$$

$$S_{1n} = \frac{2}{L}\int_0^L \sum_i e_i(z)\cos(k_0 z + \theta_i) \times \sin\left(k_L n\left(z-\frac{L}{2}\right)\right) dz \tag{23}$$

$$S_{1n} = \frac{2}{L}\int_0^L \sum_i e_i(z)\sin(k_0 z + \theta_i) \times \sin\left(k_L n\left(z-\frac{L}{2}\right)\right) dz. \tag{24}$$

The subscript index n for the coefficients C_{1n} and C_{2n} ranges from 0 to ∞. For the coefficients S_{1n} and S_{2n}, it ranges from 1 to ∞. The equation of motion for ψ neglecting the energy change can be rewritten as

$$\psi'' = \frac{\omega}{c}\frac{1}{\gamma_0^3\beta_0^3}\frac{q}{mc^2}\left(-\frac{1}{2}a_0(\psi) + \sum_{n=1}^{\infty} a_n(\psi)(-1)^{n+1} \times\cos(k_L n z) + \sum_{n=1}^{\infty} b_n(\psi)(-1)^{n+1}\sin(k_L n z)\right). \tag{25}$$

If the period of motion for a potential due to the first term in the above equation is T, and $1/T \ll k_L$, the phase ψ can be represented as a sum of a smooth motion term $\bar{\psi}$ and a fast small oscillation term. By averaging over the rapid oscillations, the equation of motion for the smooth variable $\bar{\psi}$ is given as [11]

$$\bar{\psi}'' = F_0\left(-\frac{1}{2}a_0(\bar{\psi}) - \frac{F_0}{4k_L^2}\nabla\sum_{n=1}^{\infty}\frac{1}{n^2} \times (a_n^2(\bar{\psi}) + b_n^2(\bar{\psi}))\right) \tag{26}$$

where the $\nabla = \partial/\partial\bar{\psi}$ and the constant $F_0 = (\omega/c)(1/\gamma_0^3\beta_0^3)(q/mc^2)$. This equation can be re-written as

$$\bar{\psi}'' = -\nabla U_{\text{eff}} \tag{27}$$

where the effective potential U_{eff} is given by

$$U_{\text{eff}} = A_0(\bar{\psi}) + \frac{F_0^2}{4k_L^2}\sum_{n=1}^{\infty}\frac{1}{n^2}(a_n^2(\bar{\psi}) + b_n^2(\bar{\psi})) \tag{28}$$

and

$$A_0(\bar{\psi}) = \frac{F_0}{2}(C_{10}\sin(\bar{\psi}) + C_{20}\cos(\bar{\psi}) - C_{10}\bar{\psi}). \tag{29}$$

To obtain the analytical functional dependence of the effective potential on the phase, we substitute Eqs. (19)–(24) into Eq. (28) and obtain

$$U_{\text{eff}} = U_0 + U_1\bar{\psi} + U_2\cos(\bar{\psi}) + U_3\sin(\bar{\psi}) + U_4\cos(2\bar{\psi}) + U_5\sin(2\bar{\psi}) \tag{30}$$

where

$$U_0 = \frac{F_0^2}{4k_L^2}\sum_{n=1}^{\infty}\frac{1}{n^2} \times\left(\frac{3}{2}(C_{1n}^2+S_{1n}^2)+\frac{1}{2}(C_{2n}^2+S_{2n}^2)\right) \quad (31)$$

$$U_1 = \frac{-F_0}{2}C_{10} \quad (32)$$

$$U_2 = \frac{F_0}{2}C_{20} - \frac{F_0^2}{2k_L^2}\sum_{n=1}^{\infty}\frac{1}{n^2}(C_{1n}^2+S_{1n}^2) \quad (33)$$

$$U_3 = \frac{F_0}{2}C_{10} + \frac{F_0^2}{2k_L^2}\sum_{n=1}^{\infty}\frac{1}{n^2}(C_{1n}C_{2n}+S_{1n}S_{2n}) \quad (34)$$

$$U_4 = \frac{F_0^2}{4k_L^2}\sum_{n=1}^{\infty}\frac{1}{2n^2}(C_{1n}^2+S_{1n}^2-C_{2n}^2-S_{2n}^2) \quad (35)$$

$$U_5 = -\frac{F_0^2}{4k_L^2}\sum_{n=1}^{\infty}\frac{1}{n^2}(C_{1n}C_{2n}+S_{1n}S_{2n}). \quad (36)$$

The effective potential is a nonlinear function of the phase $\bar{\psi}$. As a linear approximation, we assume that $\bar{\psi}\ll 1$, therefore the effective potential is reduced to a quadratic function of $\bar{\psi}$, i.e.

$$U_{\text{eff}} = \left(-\frac{F_0}{4}C_{20}+\frac{F_0^2}{4k_L^2}\sum_{n=1}^{\infty}\frac{1}{n^2}(C_{2n}^2+S_{2n}^2)\right)\bar{\psi}^2 \quad (37)$$

The zero-current phase advance for this potential is given by

$$\sigma_{0l} = L\sqrt{2\left(-\frac{F_0}{4}C_{20}+\frac{F_0^2}{4k_L^2}\sum\nolimits_{n=1}^{\infty}\frac{1}{n^2}(C_{2n}^2+S_{2n}^2)\right)}. \quad (38)$$

In the smooth approximation, for the slow variables $\bar{\psi}$ and $\bar{p}_t$, the longitudinal equation of motion can be written as

$$\bar{\psi}' = \frac{\omega}{c}\frac{\bar{p}_t}{\gamma_0^3\beta_0^3} \quad (39)$$

$$\bar{p}_t' = -\frac{c}{\omega}\gamma_0^3\beta_0^3\nabla U_{\text{eff}}. \quad (40)$$

From these equations, we can define a Hamiltonian,

$$\bar{H} = \frac{1}{2}\frac{\omega}{c}\frac{\bar{p}_t^2}{\gamma_0^3\beta_0^3}+\frac{c}{\omega}\gamma_0^3\beta_0^3 U_{\text{eff}}. \quad (41)$$

The phase acceptance can be found from the first positive root of $\nabla U_{\text{eff}}(\bar{\psi}^+)=0$, i.e.

$$U_1 - U_2\sin(\bar{\psi}^+) + U_3\cos(\bar{\psi}^+) - 2U_4\sin(2\bar{\psi}^+) + 2U_5\cos(2\bar{\psi}^+) = 0 \quad (42)$$

and the first negative root of

$$U_{\text{eff}}(\bar{\psi}^-) = U_{\text{eff}}(\bar{\psi}^+) \quad (43)$$

which yields

$$\Delta\bar{\psi} = \bar{\psi}^+ - \bar{\psi}^-. \quad (44)$$

The maximum energy width inside the RF bucket is therefore given as

$$|P_t|_{\max} = \sqrt{2}\frac{c}{\omega}\gamma_0^3\beta_0^3\sqrt{\Delta U_{\text{eff}}} \quad (45)$$

where ΔU_{eff} is the depth of the potential well.

3. Smooth approximation with acceleration

In the preceding section, we have assumed that the particle energy remains constant through a lattice period. The flight time of the reference particle can be written as a linear function of position z, i.e. $t_0 = (1/\beta_0 c)z$. When the effects of acceleration are not negligible, the linear dependence of flight time on position is no longer valid. Simultaneous solution of the equations of motion (Eqs. (7) and (8)) for the reference particle and the equations of motion for the charged particles (Eqs. (5) and (6)) is now required. Considering only the longitudinal motion and neglecting space-charge forces, the equation of motion for the phase is

$$\psi'' - \gamma_0^3\beta_0^3\left(\frac{1}{\gamma_0^3\beta_0^3}\right)'\psi' - \frac{\omega}{c}\frac{1}{\gamma_0^3\beta_0^3}\frac{q}{mc^2} \times\sum_i e_{0i}(z)(\cos(\omega t_0(z)+\theta_i) - \cos(\psi+\omega t_0(z)+\theta_i)) = 0. \quad (46)$$

This equation has a damping term from the first derivative of phase ψ. In this case, the smooth approximation used in the last section is no longer applicable. After defining a new variable, ϕ as

$$\phi = \sqrt{\gamma_0^3\beta_0^3}\psi \quad (47)$$

we obtain the equation of motion for ϕ as

$$\phi'' = F(\phi, z) \tag{48}$$

where

$$F(\phi,z) = \left(\frac{1}{2}a'(z) + \frac{1}{4}a^2(z)\right)\phi + \frac{\omega}{c}\frac{1}{\sqrt{\gamma_0^3\beta_0^3}} \times \frac{q}{mc^2}\sum_i e_{0i}(z)(\cos(\omega t_0(z)+\theta_i) - \cos(\phi/\sqrt{\gamma_0^3\beta_0^3} + \omega t_0(z) + \theta_i)) \tag{49}$$

and

$$a(z) = \frac{3\gamma_0'}{\gamma_0\beta_0^2} \tag{50}$$

$$a'(z) = \frac{3}{\gamma_0^2\beta_0^2}\left((\gamma_0')^2 + \gamma_0\gamma_0'' - 2\left(\frac{\gamma_0'}{\beta_0}\right)^2\right). \tag{51}$$

We can obtain the effective potential in the smooth approximation for such system following the procedure given by Channell [12]. In this procedure, we assume that the trajectory of the particle phase is the sum of a fast oscillation and a slow smooth motion. The force driving the particle motion can therefore be separated into two parts corresponding to the fast and slow motion:

$$\phi = \bar{\phi} + \tilde{\phi} \tag{52}$$

$$F(\phi, z) = \bar{F}(\phi) + \tilde{F}(\phi, z) \tag{53}$$

where $|\tilde{\phi}| \ll |\bar{\phi}|$. Substituting ϕ into $F(\phi, z)$, and neglecting high-order terms in the Taylor expansion, we obtain the equations of motion for the fast variable and the slow variable, respectively:

$$\tilde{\phi}'' = \tilde{F}(\bar{\phi}, z) \tag{54}$$

$$\bar{\phi}'' = \bar{F}(\bar{\phi}) + \tilde{\phi}\frac{\partial \tilde{F}}{\partial \bar{\phi}}. \tag{55}$$

The first term on the right-hand side of Eq. (55) is given by

$$\bar{F}(\phi) = \frac{1}{L}\int_0^L \mathrm{d}z F(\phi, z). \tag{56}$$

The second term on the right-hand side of Eq. (55) is a product of two fast variables and has both a slow and a fast component. In the equation of the slow variable, $\bar{\phi}$, we keep only the slow component of the product which is given by

$$f(\bar{\phi}) = \frac{1}{L}\int_0^L \mathrm{d}z \tilde{\phi}\frac{\partial \tilde{F}}{\partial \bar{\phi}}. \tag{57}$$

The approximate solution for the fast variable in Eq. (54) can be written as

$$\tilde{\phi}(z) = \tilde{\phi}(0) + \tilde{\phi}'(0)z + \int_0^z \mathrm{d}\tau \int_0^\tau \mathrm{d}\tau' \tilde{F}(\bar{\phi}, \tau'). \tag{58}$$

Removing the secular growth of the fast oscillation variable, we obtain the condition for $\tilde{\phi}'(0)$ as

$$\tilde{\phi}'(0) = -\frac{1}{L}\int_0^L \mathrm{d}\tau \int_0^\tau \mathrm{d}\tau' \tilde{F}(\bar{\phi}, \tau'). \tag{59}$$

Substituting $\tilde{\phi}$ into the function f, we obtain

$$f(\bar{\phi}) = \frac{1}{L}\int_0^L \mathrm{d}z\left(\frac{-z}{L}\int_0^L \mathrm{d}\tau \int_0^\tau \mathrm{d}\tau' F(\bar{\phi}, \tau') + \int_0^z \mathrm{d}\tau \int_0^\tau \mathrm{d}\tau' F(\bar{\phi}, \tau')\right)\frac{\partial \tilde{F}(\bar{\phi}, z)}{\partial \bar{\phi}}. \tag{60}$$

The equation of motion for the slow variable $\bar{\phi}$ is

$$\bar{\phi}'' = \bar{F}(\bar{\phi}) + f(\bar{\phi}). \tag{61}$$

The term $f(\bar{\phi})$ in the above equation is also called the ponderomotive force. Writing Eq. (61) in the form of the gradient of the potential, we obtain the effective potential as

$$U_{\mathrm{eff}}(\bar{\phi}) = -\int_0^{\bar{\phi}} \mathrm{d}x(\bar{F}(x) + f(x)). \tag{62}$$

From the effective potential, we can calculate the phase acceptance and maximum energy width

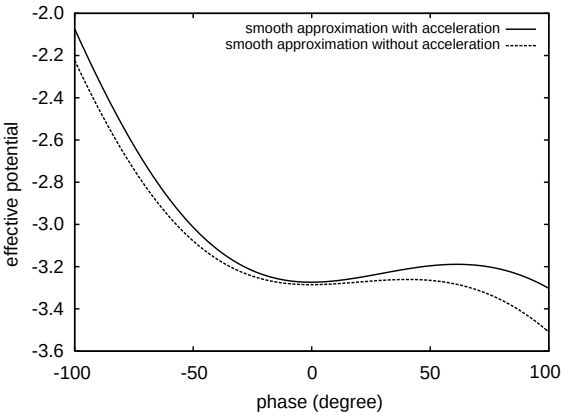

Fig. 1. Effective potential with and without acceleration as a function of phase from the smooth approximation.

following the procedure used in the last section. Fig. 1 shows the effective potential as a function of phase in the lattice to be described in Section 4. The figure shows a comparison of the effective potential with and without acceleration. Without including the effects of acceleration, the smooth approximation gives a weaker effective RF bucket, i.e. smaller phase acceptance and potential well depth, compared with the smooth approximation with acceleration. The energy gain in this case is 0.36 MeV and the zero-current phase advance is 90°. The linear zero-current phase advance can also be calculated from the linear expansion of the restoring force around zero. This gives

$$\sigma_{0l} = L\sqrt{-\frac{\partial \bar{F}}{\partial \bar{\phi}} - \frac{\partial f}{\partial \bar{\phi}}}. \tag{63}$$

Fig. 2 shows the zero-current phase advance as a function of energy gain per period by changing the RF field level in Fig. 3. At lower energy gain and phase advance, both the transfer matrix calculation [13] and the smooth approximation with/without acceleration agree well. With increasing energy gain, the phase advance difference between the smooth approximation and the transfer matrix gradually increases. However, below 90° phase advance, the smooth approximation with acceleration still gives very good agreement with the transfer-matrix calculation while the smooth approximation without acceleration underestimates the phase advance in this regime. Beyond 90° phase advance, the linear expansion used in the calculation of phase advance in the smooth approximation is no longer valid. This results in the discrepancy observed in Fig. 2. In general, the zero-current phase advance calculated from the smooth approximation with acceleration gives better agreement with the transfer matrix calculation than with the smooth approximation without acceleration.

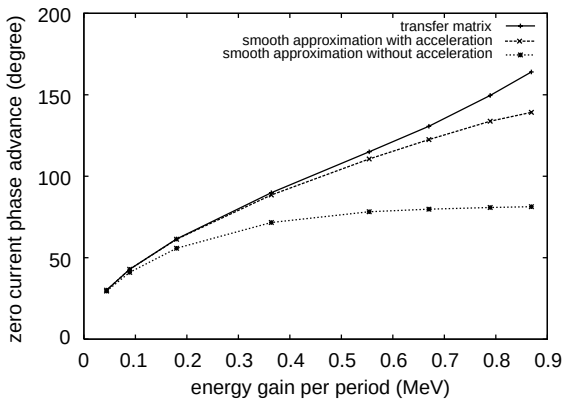

Fig. 2. Zero-current phase advance as a function of energy gain per period.

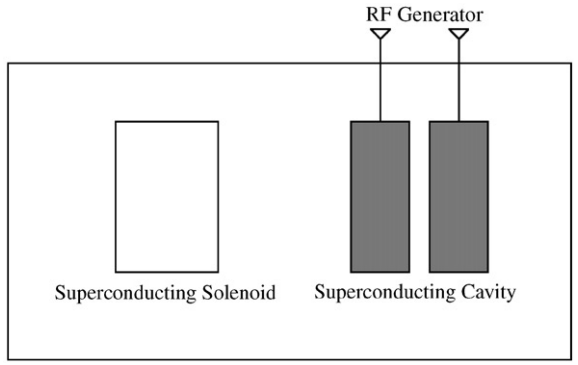

Fig. 3. Schematic plot of one period of the accelerator structure.

4. Longitudinal alternating phase focusing in a superconducting linac

The smooth approximation with acceleration has been applied to the study of longitudinal alternating phase focusing in the proposed Accelerator-Driven Test Facility (ADTF) accelerator design [14]. A schematic plot of one period of the accelerator structure is shown in Fig. 3. It consists of a superconducting solenoid for transverse focusing and two superconducting spoke-resonator RF cavities for acceleration and longitudinal focusing. By adjusting the drive phase of the two cavities, we can achieve the same acceleration but with one cavity focusing and the other cavity defocusing. This will reduce the total zero-current phase advance in one period and may avoid the envelope instability when the zero-current phase advance is greater than 90°. Using the longitudinal alternating phase focusing also reduces the magnetic field strength requirement for the external

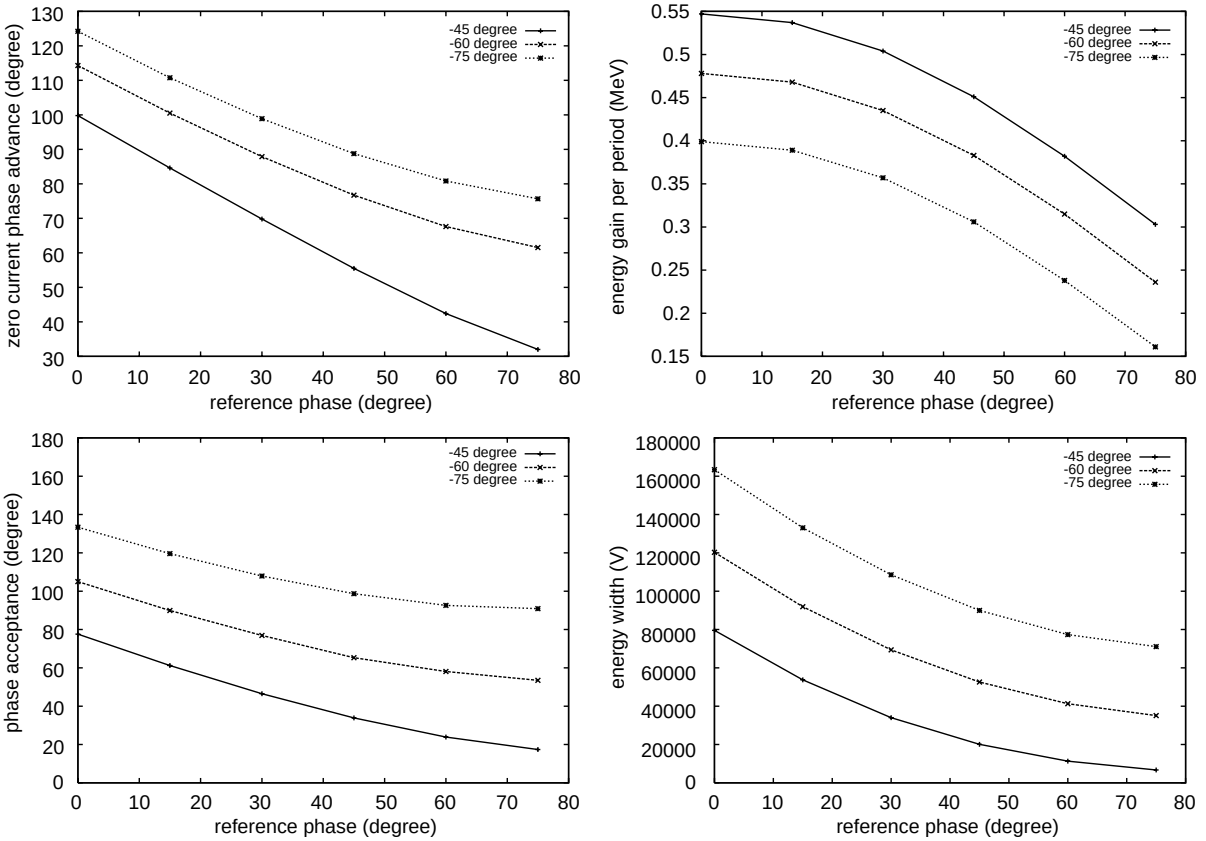

Fig. 4. Zero-current phase advance, energy gain per period, phase acceptance, energy width as a function of the reference phase in the second RF cavity for three reference phases in the first RF cavity.

transverse focusing from the solenoid. Fig. 4 shows the zero-current phase advance, energy gain per period, phase acceptance, and energy width as a function of the reference phase in the second RF cavity for three reference phases, -45°, -60°, and -75°, in the first RF cavity. The particle initial kinetic energy is 6.52 MeV. The average RF field level on the axis is 3.0 MV/m. We see that with increasing reference phase in the second RF cavity, the zero-current phase advance, energy gain per period, phase acceptance and energy width all decrease. The smaller reference phase in the first cavity gives a larger energy gain per period, but smaller phase acceptance and energy width. Given the fixed zero-current phase advance, the smaller reference phase in the second RF cavity also results in smaller reference phase in the first cavity with fixed RF field level. This will result in higher energy gain per period but lower phase acceptance and energy width. A compromise has to be made between the energy gain and the size of the RF bucket.

For a different initial input kinetic energy, the zero-current phase advance, energy gain per period, and the size of RF bucket will change. Fig. 5 shows the zero-current phase advance, energy gain per period, phase acceptance and energy width as a function of reference phase in the second RF cavity with a -60° reference phase in the first cavity and initial kinetic energies of 6.52 and 20 MeV. With high initial particle kinetic energy, the energy gain per period increases, the zero-current phase advance decreases, and the phase acceptance decreases. There is a cross-over

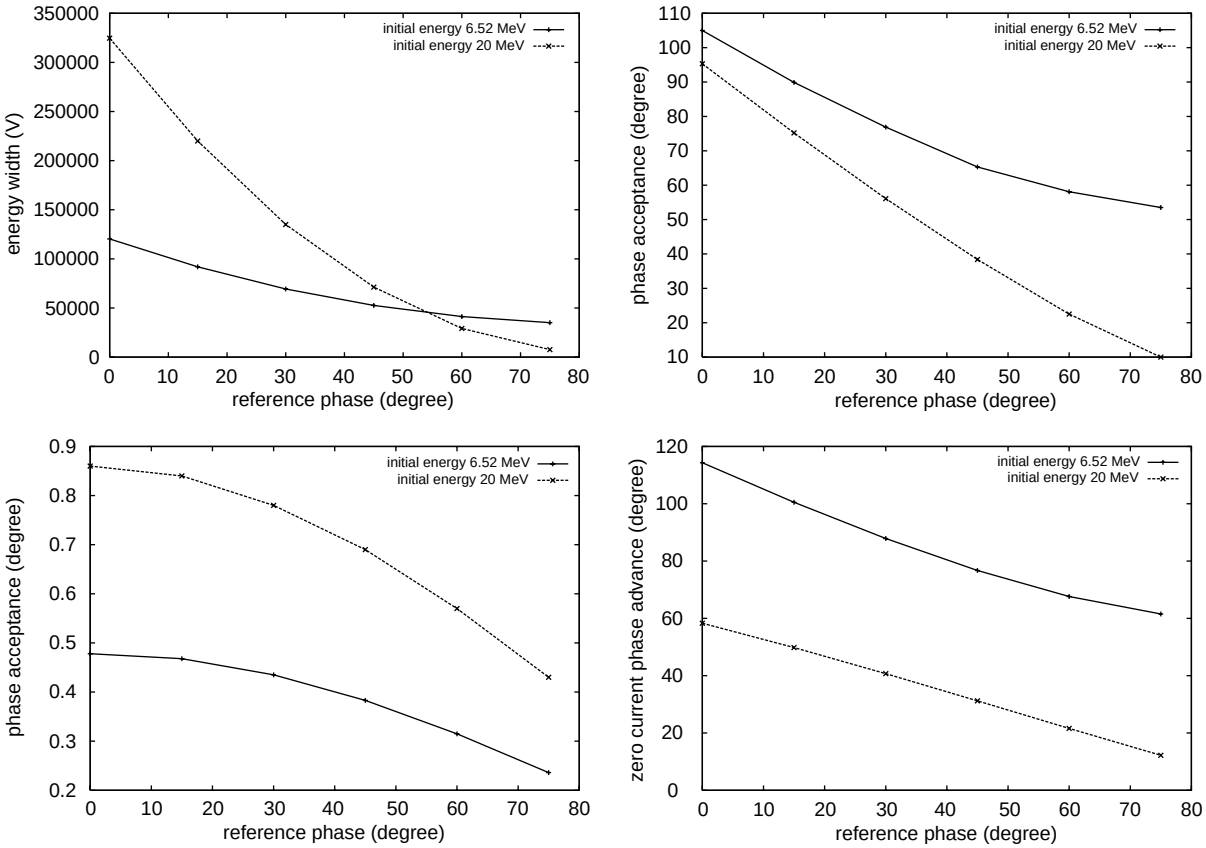

Fig. 5. Zero-current phase advance, and energy gain per period, phase acceptance, energy width as a function of the reference phase in the second RF cavity for two different initial input kinetic energies.

point for the energy width as a function of reference phase. Below this point, the higher initial energy particle will have a larger energy width and above it, the higher initial energy particle will have a smaller energy width. Since the zero-current phase advance has been significantly lowered below 90° at 20-MeV initial energy, the reference phase in the second RF cavity can be chosen towards the lower end without worrying about the potential envelope instability. This will also help to increase the energy gain per period, increase the energy width and leads to a smaller reduction of the phase acceptance.

Fig. 6 shows the zero-current phase advance, energy gain per period, phase acceptance, and energy width for average RF field levels of 3 and 5 MV/m, and an initial kinetic energy of 6.52 MeV. We see that even though the energy gain, phase acceptance and energy width have been improved with higher RF field value, the zero current phase advance also increases. For the given zero-current phase advance in the ADTF accelerator design, this limits the RF field level that can be used.

From the above parameter scanning study, we have selected one reference case with a reference phase of -75° in the first cavity and $+45^\circ$ in the second cavity. We have done self-consistent 3D macroparticle simulation using the IMPACT code [15] to find the current limit in such a structure. The initial normalized transverse emittance is 0.026 cm mrad and the longitudinal emittance is

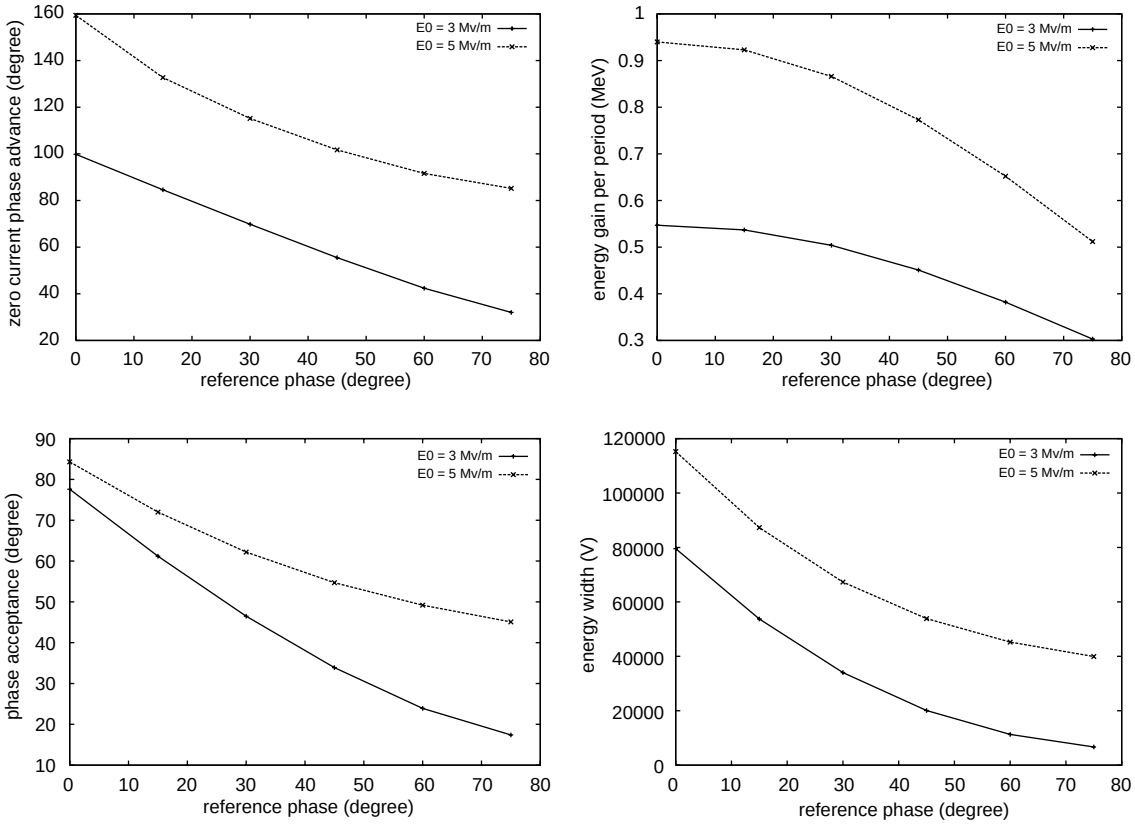

Fig. 6. Zero-current phase advance, energy gain per period, phase acceptance, and energy width as a function of the reference phase in the second RF cavity for two different average RF field levels.

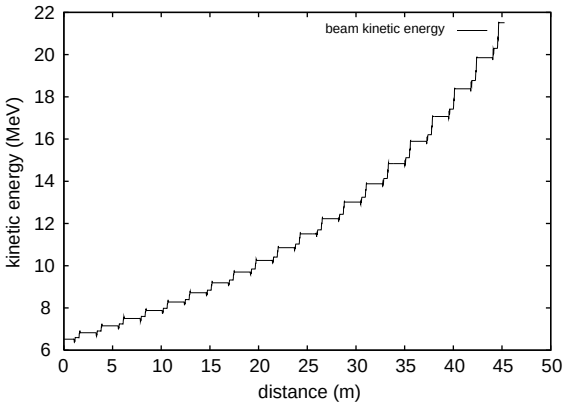

Fig. 7. Kinetic energy of the beam as a function of distance.

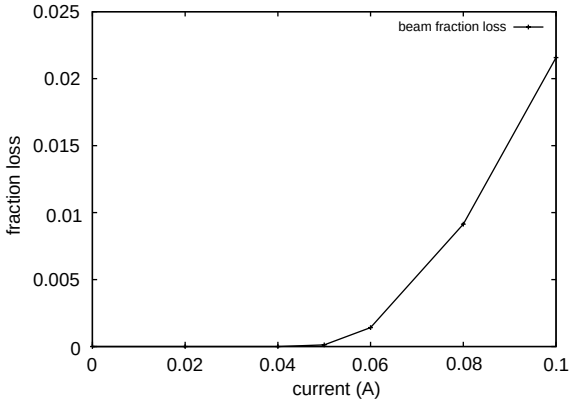

Fig. 8. The fraction of particle loss as a function of beam current.

0.17° MeV. The average acceleration gradient used here ramps up from 3 to 9 MV/m to keep the longitudinal zero-current phase advance equal to 89°. The solenoid magnetic field is also ramped from 2.16 to 2.75 T to maintain a 75° zero-current transverse phase advance. Fig. 7 shows the kinetic

energy of the beam as a function of distance through 20 periods of RF structure from the simulation. We see that after 45 m, the kinetic energy has reached 21.5 MeV. Compared with the original design based on conventional phase focusing [14], the kinetic energy has increased by 3.3 MeV. Fig. 8 shows the beam fraction loss at the end of the simulation as a function of input current. Beyond 50 mA, the particle loss increases significantly. This will put an upper boundary on beam intensity in future machine operation if the APF approach is used.

5. Conclusions

From the above study, we have shown that including the effects of acceleration in the smooth approximation to longitudinal RF focusing results in better agreement with transfer matrix calculations than the usual smooth approximation without acceleration in the calculation of zero-current phase advance. Hence, the effective potential from the smooth approximation with acceleration can be quantitatively different from that without acceleration. Using such a smooth approximation, we have studied an alternating phase focusing structure in the proposed ADTF superconducting linac by scanning the reference phase in the second RF cavity subject to different values of reference phase in the first RF cavity, namely, initial particle energy and average RF field level. Given the zero-current phase advance and the field level, there is a compromise between the energy gain per period and the size of RF the bucket in choosing the reference phases of the cavities. For a higher energy particle, the restriction of zero-current phase advance is reduced and the choice of reference phases can be done to optimize both the energy gain and RF bucket size. Raising the average field level can improve both the energy gain and RF bucket size but will also increase the zero-current phase advance which is usually limited by the envelope instability consideration. Self-consistent macroparticle simulations for an asymmetrical alternating phase focusing system with a -75° reference phase for the first cavity and a $+45^\circ$ phase for the second cavity have been completed. These results show that beyond 50 mA of beam current, there will be significant particle losses. This will put a limit on future machine operation based on the alternating phase focusing approach.

Acknowledgements

The author (JQ) would like to thank Dr. R. Ryne for reading the manuscript and instructive discussion. We would also like to thank Drs. D. Schrage, P. Channell and T. Wangler for helpful discussions and Dr. F. Krawczyk for the field data in RF cavity. This work was performed on the Cray T3E and IBM SP at the National Energy Research Scientific Computing Center located at Lawrence Berkeley National Laboratory, and the SGI Origin 2000 at the Advanced Computing Laboratory located at Los Alamos National Laboratory. This work was supported by the US Department of Energy, Office of Science, Division of High Energy and Nuclear Physics, under the project, Advanced Computing for 21st Century Accelerator Science and Technology.

References

[1] Y.B. Faynberg, Zh. Tekh. Fiz. 29 (1959) 568.
[2] V.V. Kushin, I.D. Dreval, Zh. Tekh. Fiz. 41 (1971) 598.
[3] D.A. Swenson, Part. Accel. 7 (1976) 61.
[4] H. Okamoto, Nucl. Instr. and Meth. A 284 (1989) 233.
[5] S. Minaev, U. Ratzinger, B. Schlitt, APF or KONUS drift tube structures for medical synchrotron injectors—a comparison, Proceedings of the 1999 Particle Accelerator Conference, New York, 1999, pp. 3555–3557.
[6] E.S. Masunov, N.E. Vinogradov, Phys. Rev. Spec. Top.—Accel. Beams 4 (2001) 070101.
[7] I. Hofmann, L.J. Laslett, L. Smith, I. Haber, Part. Acc. 13 (1983) 145.
[8] L. Sagalovsky, L.R. Delayen, Alternating-phase focusing: a model to study nonlinear dynamics, Institute of Physics Conference Series No. 131, Paper presented at Int. Workshop Nonlinear Problems in Accelerator Phys., Berlin, 1992.
[9] W. Cheng, R.L. Gluckstern, H. Okamoto, Phys. Rev. E 48 (1993) 4689.
[10] P.L. Morton, Particle dynamics in linear accelerators, Ph.D Thesis, Midwestern Universities Research Association, The Ohio State University, 1963.

[11] P.L. Kapitsa, Zh. Eksp. Teor. Fiz. 21 (1951) 588.
[12] P.J. Channell, A-G focusing as a pondermotive force, Accelerator Theory Note, AT-6:ATN-83-4, Los Alamos National Laboratory, March 1983.
[13] R.D. Ryne, Finding matched RMS envelopes in RF linacs: a Hamiltonian approach, Los Alamos National Laboratory Report, 1995.
[14] R.W. Garnett, ADTF superconducting linac design—viability of reducing number of spoke sections, LA-UR-01-3741, Los Alamos National Laboratory Report, 2001.
[15] J. Qiang, R.D. Ryne, S. Habib, V. Decyk, J. Comput. Phys. 163 (2000) 434.